ISSUE 10 December 2020
مجلة العلوم الإنسانية والتطبيقية
Journal of Humanitarian and Applied Sciences
العدد 10 ديسمبر 2020

Prevalence of intestinal Protozoa infection in Misurata – Libya

Faraj – Soliman El- Serite
Faculty of Medical Technology
Misurata – Libya

Altaher Aljhemi
Faculty of Arts and Sciences
Kasr-khiar

Corresponding E. mail: *Farg9958@yahoo.com*

الملخص

أجريت دراسة بمدينة مصراته بغرب ليبيا على عدد 394 مريض منهم 185 ذكور و 209 إناث، كانوا قد ترددوا على مختبر مصراته المركزي خلال العام 2018 للكشف عن بالطفيليات الأولية، حيث أظهرت النتائج كالتالي:

معدل نسبة الإصابة العام (69) 19.77% بالطفيليات الأولية أما نسبة الإصابة بالطفيليات فكانت النتائج *Entamobe histolytica, Giardia lamblia* و 3.2% بـ *Entamobe coli* .إصابة 6.3% بطفيلُ بـ 0.76% أما من حيث الجنس فكانت نسبة الإصابة بالإناث 10.4% وبالذكور 7.10% ، كما أعطيت التحاليل الإحصائية لقيمة $p-value = (P < 0.515)$, $(p < 0.085)$ و ظهرت بعض الحلات المرضية علي المصابين مثل الأنيميا و الإسهال (P<0.086)

Abstract

The study was carried out within the period of January to June 2018. at Misurata Central laboratory A total of 394 patients attending clinics and admission were recruited for this study the consisted of (185) males and (209) of females.

Age group between 1-40 years.

The results: out of 394 samples analyzed (209 females, 185 males) in Misurata Central laboratory (2018) : 69(19.77%) stool samples were positive for cysts.

The common parasite was *Entamobe coli* 6.3% followes by *Entamobe histolytica* 3.2% and *Giardia lamblia* 0.7%, the response rate of males was 28(7.10%) and 41 cases (10.4%) rate was seen in females (P<0.515) some cases with parasites disease ex anemia and dirrah (P<0.086)

Keywords: intestinal protozoa , parasites pathogenic Misurata – Preralence

Introduction

Intestinal parasite infections are among the most common infections worldwide. It is estimated that approximately 3.5 billion people are affected and that 450 million are ill as a result of these infections, the majority being children (Okyay 2004) common intestinal parasites such as *Blastocystis hominis* and *Giardia lamblia* are still healty *challenges* of economically developed and developing countries (Hill 2007) . The prevelence of *Blastocystosis* in humans has

been reported to be higher in developing countries (30-50%) than in developed countries (1.5-10%) and that *B. hominis* is the most common parasite in stool specimens in symptomatic and asymptomatic presons in a. blia variety of settings (Hill, 2007).

In resource – poor countries of the world, *Giardia lamblia* is one of the first enteric pathogens to infect inflants with peak prevalence of 15-30% occurring in children younger than 10 years.

(Hill 2007). Amoebiasis due to infections with the interstinal protozoon *Entamobe histolytica* results in 40000 – 100.000 deaths each year (Chark 1997). Giardiasis caused by *Giardia duodenlis* , is the most predomimnant protoza infection with an estimated prevalence rates ranging from 2.0 to 7.0% developed countries and 20.0 to 30.0% in most developing countries (Mineno 2003) intestinal parasitic infections (IPIS) are distributed virtually throughout the world. According to the World Health Organization (WHO). (Desta 2014).

The aim of the study:

Is to investigate the rate of the natural prevalence of different protozoan parasites that infected people in the west of Libya.

Materials and Methods:

The study was carried out with in the period of January to June 2018. at the Misurata. A total of 394 patients attending clinics and admission. were recurited for this study, the consisted of (185) males and (209) of females with age rangling from 1– 40 years stool samples were collected from each patient with signs and symptoms of diarhea into clean wide – mouthed container. The samples were examined microscopially for cysts of protozoa using saline and Iodine mounts on grease – free slides . (Garcia 2001)

Data analysis (SPSS System).

The frequency data were compared using the [Chi - square test.

Results and Discussion

Table (1) Prevalences of intestinal protozou in Misurata Center Laboratory (2018)

	Parasite				
Sex	***E. coli***	***E. histolytica***	***G. lamblia***	**Non**	**Total**
F	**25**	**13**	**3**	**168**	**209**
M	**15**	**9**	**4**	**157**	**185**
Total	**40**	**22**	**7**	**325**	**394**

(P< 0.515)

Table (2) cases with parasites disease

Sex	**Complication**			
	anemia	**Dirrah**	**Non**	
F	**0**	**3**	**206**	**209**
M	**2**	**0**	**183**	**185**

(P< 0.086)

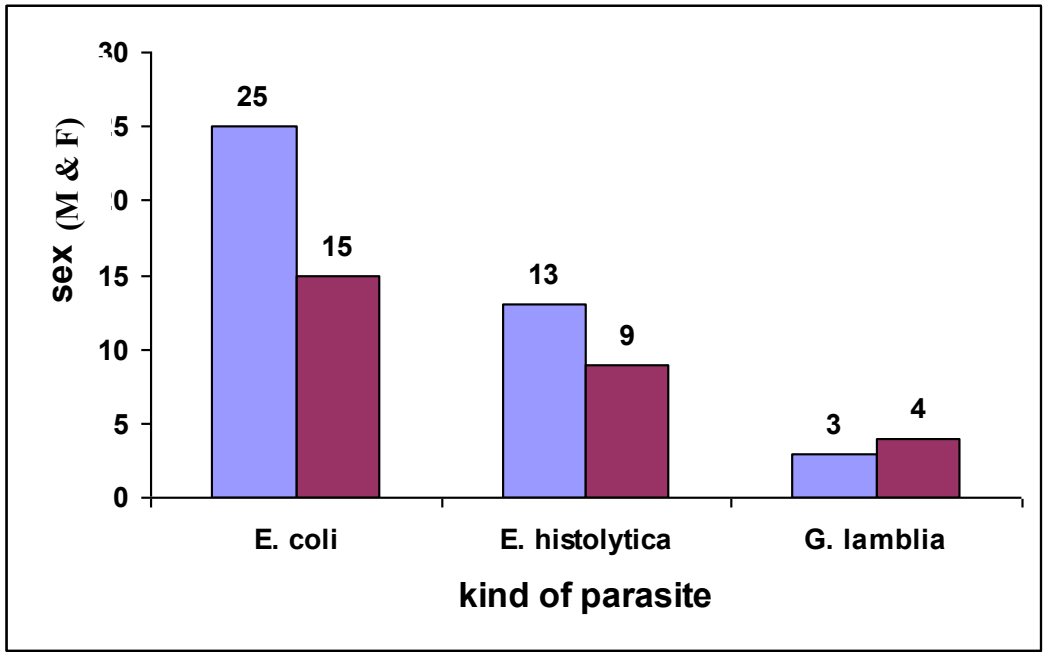

Fig(1)

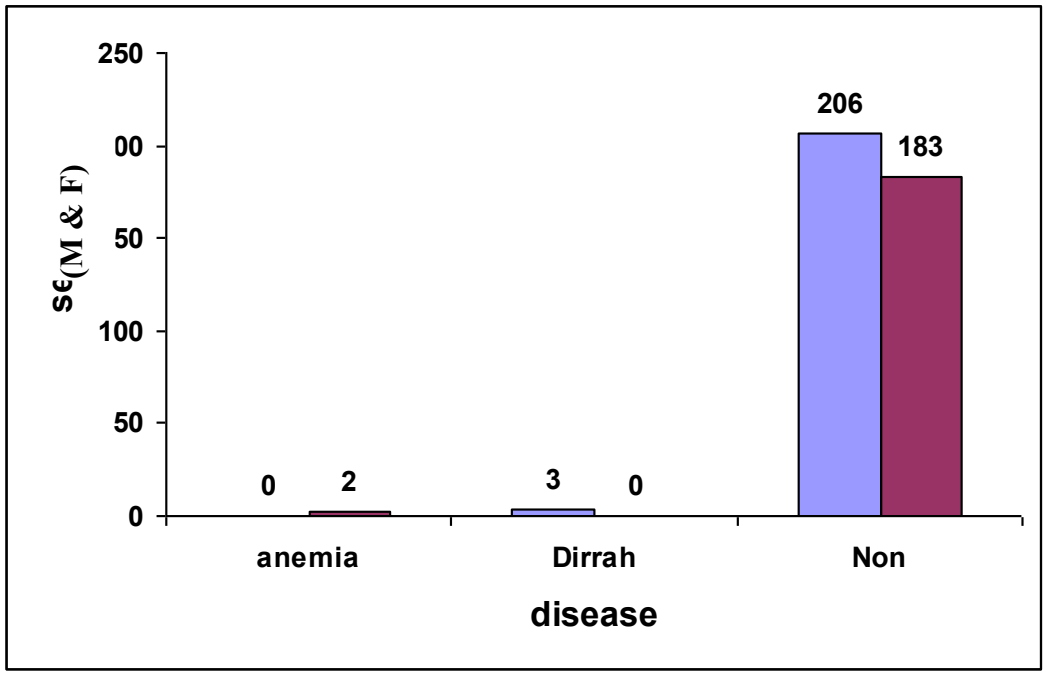

Fig(2)

Table (1) out of 394 samples analyzed (209 females, 185 males) in , 69(19.77%) stool samples were positive for cysts. The most common parasite was *Entamobe coli* 25(6.3%) followed by *Entamobe histolxytica* (3.2%) and *Giardia lamblia*.3(0.76%) 41 cases (10.4%) rate was seen in females. Fig(1)
The response rate of males was 28 (7.10%) and in females

Table (2) In males (2 cases for anemia) and (zero cases for dirrah) In females (zero cases for anemia and 3 cases for dirrah). Fig(2)

Discussion.

A total of 394 patients with suspected intestional parasites were refred to the Misurata central laboratory including (185 males + 209 females) were Laboratory diagnosed. The overall prevalence of intestinal protozoan (19.77%) in Iran a total of 4371 referred patients were laboratory diagnosed with intestinal parasites with a period of *B. hominis*, *G. lamblia* laboratory and *E. histolytic*. The percentage of infection (54.5-25.8-1.1%) respectively. (Abolfath 2008) In South Africa. A total of 162 learnvers stool samples were examined the prevalemce of parasites (9.9% *G. lamblia*) 6.8% *E. histolytica* + 26.0% *E. coli*) (Nxasana 2013) The pathogenic protozoan *G. lamblia* a to be more prevalent in rural leamers than which correlate with (Ouattara 2012). In Southern Ethiopia the overall prevalence of intestional parasites was 27.7% the predominant parasite was *E. histolytica/diepar* 12.9% followed by *G. lamblia* 4.2% and *H. nana* 4.2% (Desta 2014), females (51.4%) had slightly higher overall prevalence rate compared to male 48.6% which is in line a study reported in Misurata (Ngui 2011) and Nepal (Sah 2013) *G. lamblia* is highly infections parasite capable causing gastrointestinal illness in bot human and Malaysia *G. Lamblia* infection was higher in males (4.7%) than in females (2.0%) (Suman 2011). The prevalence of intestinal parasitic infections in Sharzah) (U.A.E). The rate of infection in males (58%) was hogher than on females (42%) Overall protozoa infections (92.2%), were higher than the helminth infections (7.8%), *E. histolytica* (71.8%) and *G. lamblia* (17.5) (Nihar, 2010). These studies its similar to our study

In Western Iran. The results showed 9.0 stool specimens were positive for different intestinal parasite ex. *G,.lambila* 2.9% *E.coli* 4.3% and *Blastocystis* sp 1.4% (Faranaz 2014)

In Ghana The overall prevalence of protozoan among studied school children was 42.9% prevalence was significantly higher in males than females. The highest Protozoa Infection was *G. lamblia* 16.8% followed by *E. histolytica* (2.2 and E. coli 8.5% (Williams 2014).

In Sudan; prevalence of intestional coccidiam parasites immuniocompromised patients, in males and females was almost the same (31.5 and 32.0% respectively (Khidir 2013). In Karachi, out of 22120 sample 274 (12.4%) were positive. The most prevalence protozoan was *E.histolytica* 66.1% followed by *G.lamblia* 22.3% (Salva Arshad *et al* 2019).

Acknowledgements

We thank all nurses who partocipated in this study and Dr. Amehmed Abo-Katala for his assistance with the statistical analysis.

References

1. Abolfath Shojaei ARANI Reza ALAGHEBANBAN Lame AKLAGI, Maryam Shahi and Abdolaziz Rastegar LARI, (2008).Prevalence of intestinal parasites in a

population in sout of Tehran-Iran. Rev. Inst Med. Trop. S. Paulo so(3): 145-149 May-June (2008).

2. Chark ER. DiamondI,(1997). WHO NEWS and activities Bulletin of the World Health Organization 75(3): 291-2.

3. Desta Haffu, Negussic Deyessa, Eskzyiew Agedew,(2014). Prevalence and determinant factors of intestinal parasites amony school children in Arba Minch town, Southern Ethiopoa. American Journal of Health Research 2(5): 247-254.

4. Faranaz Kheirandish,(2014). Prevalence of intestinal parasites among food hana;ers in wester Iran. Journal list. Rev. Inst. Med Trop. Sab Paulo V. 56(2) Mar Apr 2014.

5. Garcia LS,(2001). Diagnostic Medical Parasitology. Ed. 4, ASM. Press Washington, D.C.

6. Hill I. DR,(2007). *Giardia lumblia*. In Mandeli; GL. Bennet; JE Dolin, B principle and practice of infections diseases, 6. ed. New York , churechill Livingstone, P. 2888-2893.

7. Khidir, M. M, Asha, A. A. Saad M. B,(2013). Prevalence of intestinal *Coccidian* parasites in immunocomp romised patients. Sud Med Lab J: 2(1) 13-20.

8. Mineno T, Avery M,(2003). Giardiasis recent progress in chemotherapy and drug development curr pharm Design, (11): 814-55.

9. Ngui R. Ishak S, Chuen CS, Mahmud R, Lim YAL,(2011). Prevalence and Risk Factors of intestinal parasitism in Rural and Romote West Malaysis Plos Negl Trop Dis. 5(3)

10. Nihar Dash, Manzour Al-zarouni, Khurshid Anwar and Debadatta Panigrahi,(2010). Prevalence of intestinal parasitice infections in Sharjah Human parasitic Diseases: 221-24.

11. Nxasana, K. Baba, VG Bhat and SD Vasakar,(2013). Prevalence of intertial parasites in primary school children of Mthatham Eastern cape Province, South Africa. Ann Med Health Sci Res. Oct-Dec 3(4) 511-516.

12. Okyay P, Frtug S; Gultekin B, Onen O; Beser E.(2004). Intestinal parasitic prevalence and related factors in school children, a western city sample – Turkey BMC Public Health, 4: 64. [PMC free article]. [Pub Med].

13. Ouattara M. N. guessan NA, Yapi A, N goran EK,(2010). Prevalence and spatial distribution of *Entamoeba histolytica* / *dispar* and *Giardia lamblia* among school children in A gboville area (cote ivoure) Plos Negl. Trap. Dis: 4(suppl): e574. [pub Med] coted.

14. Sah R, Paudel J, Baral R; Poudel P, Jha N; Pokharel P,(2013). Prevalence of intestinal Helminthic infections of community Health; 25(2): 134-9.

15. Suman, M. S. H. MM. Alam, S. B. Pun, A. khair, S. Ahmed and R. Y. Uchida,(2011). Prevalence of *Giardia Lambila* infection in children and calves in Benyladesh Bungl. J. Vet. Med (2) : 177-182.

16. Williams Walana, Samuel Crowther Kofi Tay, Philip Tette and Juventus Benogle Ziem,(2014). Prevalence of intentional protozoan infestation among primary school children in Urban and Peri-urban communities in Kumasi – Ghana. Scince Journal of Public Health; 2(2): 32-57.

17. Salva Arshad, Nasir Khatoon, Aly Khan, Jawed Abubaker wareind, (2019). The prevalence of human intestinal protozoal and helminthic infection. Int.J.Biol. Biotech in Karachi, 16(2):319-323.

ISSUE 10 December 2020
مجلة العلوم الإنسانية والتطبيقية
Journal of Humanitarian and Applied Sciences
العدد 10 ديسمبر 2020

Numerical solutions to nonlinear Schrödinger equations in silicon waveguides

Nesreen U. ben Uounis, Prof. Mohamad A. Mansor, Prof. Abdulbaset A. Abuazza
University of Tripoli, Faculty of Science – Physics Department

Abstract

This research studies the most important properties of electromagnetic waves and waveguides as a means to transferring information, communications and various applications, and the importance of nonlinear equations and there solutions which represent Solitons or unilateral waves, and how to get solutions of the nonlinear Schrodinger equation where it will describe its optical picoseconds pulse spread in silicon waveguides, and the importance of silicon semi-conductor crystal and their features that enable them to interact with efficient nonlinear optical waves in the relatively low levels of electricity and distress.

This paper shows the use of numerical solutions to nonlinear Schrödinger equations with finite difference method to solve, and graph the illustrations and comparisons to this topic using the experimental results of previous studies, to estimate various parameters needed for these solutions.

Introduction:

Electromagnetic waves consist of a combination of oscillating electrical and magnetic fields, perpendicular to each other and perpendicular to the direction of energy and wave propagation. Although they seem different, radio waves, microwaves, x-rays, and even visible light are all electromagnetic waves. They are part of the electromagnetic spectrum, and each has a different range of wavelengths, which cause the waves to affect matter differently. [1]

James Maxwell first formally postulated electromagnetic waves in 1864[2]. These were subsequently confirmed by Heinrich Hertz. Maxwell derived a wave form of the electric and magnetic equations, thus uncovering the wave-like nature of electric and magnetic fields, and their symmetry. Because the speed of electromagnetic waves predicted by the wave equation coincided with the measured speed of light, Maxwell concluded that light itself is an electromagnetic wave.

Maxwell's equations are a set of partial differential equations that, together with the Lorentz force law, form the foundation of classical electrodynamics, classical optics, and electric circuits. These fields in turn underlie modern electrical and communication technologies.[3]

Electromagnetic waves travel in vacuum or in any homogeneous medium in the form of straight lines, but may be subject to a number of phenomena as they travel from one medium to another medium, such as reflection, refraction, diffraction and dispersion.

As electromagnetic wave travels from one medium to another, parting them regular and not curvy interface, part of this wave will be reflected to the first medium and the reflection angle will equal the angle of incidence. The remaining part of the wave will travel to the second medium, moving in refracted path, where the angle of refraction of angle of incidence combine with refraction coefficients (refractive index) for both mediums according to the law of Snell.

On the other hand, as the electromagnetic wave falls on curvy surface, the reflection will not be in one direction, but in multiple directions and this is called the phenomenon of dispersion. Furthermore, as the wave falls on a body with dimensions less than the wavelength of this wave, then the wave not be affected by the existence of the body but would deviate and continue travelling its course, and this is known as the phenomenon of diffraction. [2]

The propagation of electromagnetic waves can be broadly classified into guided and unguided propagation. In guided propagation the waves are transmitted from one point to another following a prescribed path. In unguided propagation the waves are spread or radiated in an open space.

Waveguides have undergone considerable development in the last few decades. Thus, besides the simple two copper wire lines, the coaxial cable and the hollow metallic pipes that have been used for many years, there are, in addition, the planer strip, microstrip lines, the various millimetric waveguides and the now popular optical fiber lines. The basic objective of any of these types remains almost the same.[4]

Typical examples of such structures used in guiding waves are transmission lines and waveguides. The transmission lines are mainly of two types such as two wire transmission lines and co-axial transmission lines. In case of two wire transmission line, two parallel conducting wires are separated by a uniform distance. In two wire transmission line wave guiding, the fields are guided or directed by two wires. In case of coaxial transmission line, two concentric conductors are separated by a dielectric medium. This type of the guiding structure has the advantage of restricting the electric and magnetic fields entirely within the dielectric region. Another means of guiding the waves is by the means of waveguide or tube. In waveguide, the field energy propagates inside a tube. The tube used of is either rectangular or cylindrical type without central conductor.

Waveguides are classified into two classes; closed waveguides and open waveguides. Closed waveguides are characterized by being completely bounded with perfectly, or at least highly, reflecting boundaries. Open waveguides, on other hand are not completely bounded. [5]

Types of nonlinear Wave equations

In this section we will describe the nonlinear wave equation, and there are many different types of it, some types of these equations have solutions that display singularities or gradient blow-ups, while other types of equations have

smooth dispersive solutions (decaying in time and space) or, in some cases, stable travelling wave solutions. [6]

Many exactly solvable models have soliton solutions, including the KdV equation, the nonlinear Schrödinger equation, the coupled nonlinear Schrödinger equation, and the sin-Gorden equation. Soliton or solitary wave is a localized wave propagates without change of its properties, and it is condition known in hydrodynamics since the 19th century. [7]

Then we are heading to the characteristics of the silicon crystal, the electronic states of crystals are described by the band theory of solids. The distinction between an insulator and a semiconductor is related to the size of the band gap. The band gap generally refers to the energy difference (in electron volts) between the top of the valence band and the bottom of the conduction band in insulators and semiconductors. [8]

Other thing about silicon crystal is Silicon photonics which is an evolving technology in which data is transferred among computer chips by optical rays. Optical rays can carry far more data in less time than electrical conductors. [9]

Wave propagation in nonlinear media

During the 1990s, a major factor behind such a sustained growth was the advent of fiber amplifiers and lasers, made by doping silica fibers with rare-earth materials such as Erbium and Ytteryium. Erbium-doped fiber amplifiers revolutionized the design of fiber-optic communication systems, including those making use of optical solitons, whose very existence stems from the presence of nonlinear effects in optical fibers [10]. Optical amplifiers permit propagation of light wave signals over thousands of kilometres as they can compensate for all losses encountered by the signal in the optical domain. At the same time, fiber amplifiers enable the use of massive wavelength-division multiplexing, a technique that led by 1999 to the development of lightwave systems with capacities exceeding 1 Tb/s. Nonlinear fiber optics plays an important role in the design of such high-capacity lightwave systems. In fact, an understanding of various nonlinear effects occurring inside optical fibers is almost a prerequisite for a lightwave-system designer. [11]

Starting around 2000, a new development occurred in the field of nonlinear fiber optics that changed the focus of research and has led to a number of advances and novel applications in recent years. Several kinds of new fibers, classified as highly nonlinear fibers, have been developed. They are referred to with names such as microstructured fibers, holey fibers, or photonic crystal fibers, and share the common property that a relatively narrow core is surrounded by a cladding containing a large number of air holes.[12]

The nonlinear effects are enhanced dramatically in such fibers. In fact, with a proper design of microstructured fibers, some nonlinear effects can be observed even when the fiber is only a few centimetres long. The dispersive properties of such fibers are also quite different compared with those of conventional fibers,

developed mainly for telecommunication applications. Because of these changes, microstructured fibers exhibit a variety of novel nonlinear effects that are finding applications in the fields as diverse as optical coherence tomography and high-precision frequency metrology [10].

Nonlinear Optics:

Nonlinear optics is the branch of optics that describes the behaviors of light in nonlinear media, that is, media in which the polarization P responds nonlinearly to the electric field E of the light. This nonlinearity is typically only observed at very high light intensities [13].

Nonlinear optics gives rise to a host of optical phenomena:

Second-order nonlinear processes:

There is a number of nonlinear optical phenomena can be described as second-order nonlinear processes.

1 Second harmonic generation (SHG), or frequency doubling, when light of well-defined wavelength hits a surface, a small percentage of photons might "clash" together when returning from nonlinearities of the surface material, forming a wavepacket of double the energy (half the wavelength) of the incoming photons. This is the SHG signal that corresponds to greater resolution than the incoming photons.

2 Sum and Difference-frequency generation and Parametric amplification, the Sum Frequency generation is the process in which light beams at two frequencies interact in some special conditions to produce light at a new frequency equal to the sum of the interacting frequencies $(\omega_3 = \omega_1 + \omega_2)$. In difference-frequency generation (DFG), two input fields with frequencies $\omega 1$ and $\omega 2$ generate a nonlinear signal at the frequency$(\omega_3 = \omega_1 - \omega_2)$. The Parametric amplification of a signal input in the presence of a higher-frequency pump wave, at the same time generating an idler wave [10,14].

Third-order nonlinear processes:

Optical nonlinearity of the third order is a universal property, found in any material regardless of its spatial symmetry. This nonlinearity is the lowestorder nonvanishing nonlinearity for a broad class of centrosymmetric materials, where all the even-order nonlinear susceptibilities are identically equal to zero for symmetry reasons. Third-order nonlinear processes include a vast variety of processes:

1 Self-phase modulation (SPM), the third-order nonlinearity gives rise to an intensity dependent additive to the refractive index:

$n = n_0 + n_2 I(t)$,

where n_0 is the refractive index of the medium in the absence of light field,

$n_2 = (2\pi/n_0)^2 x^{(3)}(\omega;\omega,\omega,-\omega)$ is the nonlinear refractive index, $x^{(3)}(\omega;\omega,\omega,-\omega)$ is the third-order nonlinear-optical susceptibility, and *I* (*t*) is the intensity of laser radiation.

Thus, self-phase modulation results in spectral broadening of a light pulse propagating through a hollow fiber. This effect allows compression of light pulses through the compensation of the phase shift acquired by the pulse in a hollow fiber.

2 Temporal Solitons, the nonlinear phase shift acquired by a laser pulse propagating through a medium with Kerr nonlinearity can be balanced by group-velocity dispersion, giving rise to pulses propagating through the nonlinear dispersive medium with an invariant or periodically varying shape: optical solitons (a special class of solutions to the nonlinear Schrödinger equation).

3 Cross-phase modulation (XPM), is a result of nonlinear-optical interaction of at least two physically distinguishable light pulses related to the phase modulation of one of the pulses (a probe pulse) due to the change in the refractive index of the medium induced by another pulse (a pump pulse).

Similarly, to self-phase modulation, cross-phase modulation can be employed for pulse compression. The dependence of the chirp of the probe pulse on the pump pulse intensity can be used to control the parameters of ultrashort pulses.

4 Four-Wave Mixing, In general-type four-wave mixing is three laser fields with frequencies ω_1, ω_2, and ω_3 generate the fourth field with a frequency $(\omega_{FWM} = \omega_1 \pm \omega_2 \pm \omega_3)$. In the case when all three laser fields have the same frequency $(\omega_{FWM} = 3\omega)$.

5 Optical Phase Conjugation, it is generally understood as the generation of an optical field with a time-reversed wave front, or with a conjugate phase. This effect can be used to correct aberrations in certain types of optical problems and systems.

6 Stimulated Raman scattering, vibrations or rotations of molecules, electronic motions in atoms or collective excitations of matter can interact with light, shifting its frequency through an inelastic scattering process by the frequency Ω of Raman-active motions. This phenomenon was discovered by Raman and Krishnan and almost simultaneously by Mandelstam and Landsberg in 1928. In an intense laser field, pump laser photons and frequency-shifted photons act coherently to resonantly drive molecular motions, leading to the amplification of the Raman-shifted signal. This effect is called stimulated Raman scattering (SRS).

7 Third harmonic generation (THG), generation of light with a tripled frequency (one-third the wavelength) (usually done in two steps: SHG followed by SFG of original and frequency-doubled waves). [10, 15,16,17]

Other nonlinear processes:

1 Optical Kerr effect, The Kerr effect or the quadratic electro-optic effect (QEO effect) is a change in the refractive index of a material in response to an electric field. It is distinct from the Pockels effect in that the induced index change is directly proportional to the square of the electric field instead of to the magnitude of the field. All materials show a Kerr effect, but certain liquids display the effect more strongly than other materials do. The Kerr effect was found in 1875 by John Kerr, a Scottish physicist. The refractive index (or index of refraction) of a medium is a measure for how much the speed of light (or other waves such as sound waves) is reduced inside the medium.

The Pockels effect, or Pockels electro-optic effect, produces birefringence in an optical medium induced by a constant or varying electric field. Two special cases of the Kerr effect are normally considered: the Kerr electro-optic effect, or DC Kerr effect, and the optical Kerr effect, or AC Kerr effect.

2 Stimulated Brillouin scattering (SBS), is a nonlinear process that can occur in optical fibers at input power levels much lower than those needed for stimulated Raman scattering (SRS). It manifests through the generation of a backward-propagating Stokes wave that carries most of the input energy, once the Brillouin threshold is reached. Stimulated Brillouin scattering is typically harmful for optical communication systems. At the same time, it can be useful for making fiber-based Brillouin lasers and amplifiers.

3 Two-photon absorption (TPA), is the simultaneous absorption of two photons of identical or different frequencies in order to excite a molecule from one state (usually the ground state) to a higher energy electronic state. The energy difference between the involved lower and upper states of the molecule is equal to the sum of the energies of the two photons. Two-photon absorption is a third-order processes several orders of magnitude weaker than linear absorption. It differs from linear absorption in that the strength of absorption depends on the square of the light intensity, thus it is a nonlinear optical process.

4 Multiple photoionization, the first studies of multiple photoionization of free atoms was made about 1923 by Auger. He used a Wilson cloud chamber filled with argon gas at about 1 atm. pressure, through which he passed x-rays with energies in the 20 keV range. He observed numerous small tracks surrounding the starting point of the larger photoelectron track. After a series of experiments, he observed that the small tracks always had the same length regardless of the x-ray energy that was used. However, the length of the photoelectron track was a function of the x-ray energy. [15,16,17,18]

Numerical Calculation

Single Solitons:

Theory and numerical technique

In this work, the form of the nonlinear Schrödinger equation is obtained from equation

$$i\frac{\partial A}{\partial z}+\frac{i\alpha}{2}A-\frac{\beta_2}{2}\frac{\partial^2 A}{\partial T^2}+\gamma|A|^2A=0.$$

$$i\frac{\partial F}{\partial z}+i\frac{\alpha}{2}F-\frac{\beta_2}{2}\frac{\partial^2 F}{\partial t^2}+\gamma|F|^2F=0 \qquad (4.1.1)$$

Where F is the amplitude of the soliton

α is waveguide linear loss

β_2 group velocity dispersion

And

$$\gamma=\gamma_1+i\gamma_2=\frac{n_2}{\lambda A_{eff}}+i\frac{\beta_{TPA}}{2A_{eff}} \qquad (4.1.2)$$

n_2 is the nonlinear Kerr index coefficient, A_{eff} is the effective cross section of the waveguide and β_{TPA} is the two photon absorption coefficient.

With initial conditions

$$F(z,0)=f(z) \qquad (4.1.3)$$

and boundary conditions

$$\frac{\partial F(z,t)}{\partial z}=0 \ , \ at \qquad z=z_1=z_2 \qquad (4.1.4)$$

for our numerical work, we decompose the complex function F into their real and imaginary parts by writing

$$F(z,t)=A(z,t)+iB(z,t) \qquad (4.1.5)$$

where $A(z,t)$, $B(z,t)$ are real functions. By substituting equations (4.1.5) and (4.1.2) into equation (4.1.1), we can obtain two systems

$$-\frac{\partial(A+iB)}{\partial z}=-\frac{\alpha}{2}(A+iB)+i\frac{\beta_2}{2}\frac{\partial^2(A+iB)}{\partial t^2}$$

$$-i(\gamma_1+i\gamma_2)|A+iB|^2(A+iB)$$

$$\frac{\partial A}{\partial z}=-\frac{\alpha}{2}A+\frac{\beta_2}{2}\frac{\partial^2 B}{\partial t^2}-(A^2+B^2)[A\gamma_2+B\gamma_1]. \qquad (4.1.6)$$

$$\frac{\partial B}{\partial z}=-\frac{\alpha}{2}B-\frac{\beta_2}{2}\frac{\partial^2 A}{\partial t^2}-(A^2+B^2)[B\gamma_2-A\gamma_1]. \qquad (4.1.7)$$

In order to develop the numerical solution for the system in equations (4.1.6) and (4.1.7), the space domain is between $[z_1, z_2]$ is divided into a large number of nodes at the coordinates

$$z_n = nh \quad , \; n = 0,1,2, \dots N \qquad (4.1.8)$$

where *h* is the space separation between adjacent nodes.

The time domain is also divided into small intervals of length *k* such that

$$t^m = mk \quad , \; m = 0,1,2, \dots M \qquad (4.1.9)$$

To second order in h, the space derivatives are evaluated by the finite difference method

$$\frac{dF}{dz} = \frac{F_{n+1}^m - F_{n-1}^m}{2h}$$

$$\frac{d^2F}{dz^2} = \frac{F_{n+1}^m + F_{n-1}^m - 2F_n^m}{h^2}$$

To propagate the solution in to space, we introduce a computer program to solve the nonlinear Schrödinger equation in space domain numerically. This program is based on fourth order Runge_Kuta method, and is shown in Appendix(I).

The first step is to calculate the input signal pulse which has a Gaussian shape with two parts, real part and imaginary part using the subroutine sig(k,M).

The signal profile is at $(z = 0)$ as a function of discretized time as shown in figure (4.1). This profile is fed into the subroutine called Integ and N steps in space are carried by using Runge_Kuta method. Then the result is fed into the subroutine Auv to get the absolute values of the signal which is easily graphed as two-dimensional surface plots.

Numerical Results

To investigate the performance of the proposed scheme, the first step is to assume a specific shape for the signal pulse, we choose the Gaussian shape of the form

$$A(0, t_m) = A_0 exp\left[-\frac{(t_m - t_0)^2}{2\delta^2}\right] \qquad (4.1.10)$$

Where δ, A_0 and t_0 are constants.

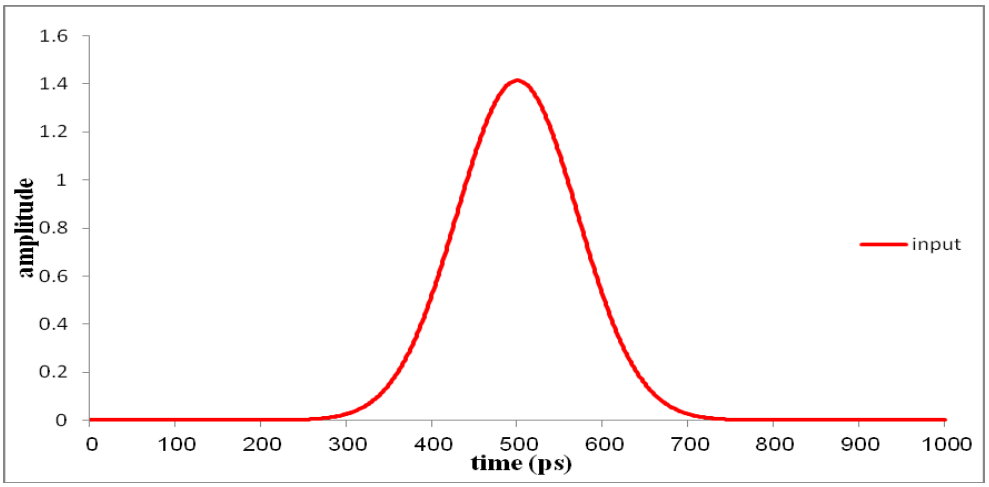

Figure (4.1): the input wave Gaussian shape.

The next step, we will inter a Gaussian shape [figure (4.1)] in silicon on insulator waveguide at $\lambda = 1550nm$ and I use the parameters from table (1) [46…51] in my calculation.

Table (1): values of the parameters for SOI waveguides used for numerical calculations.

Values	(1) [46,47]	(2) [48,49]	(3) [50,51]
$A_{eff}\ (m^2)$	0.37×10^{-12}	0.38×10^{-12}	0.4×10^{-12}
$n_2\ (m^2/W)$	6×10^{-18}	4.4×10^{-18}	6×10^{-18}
$\beta_{TPA}(m/W)$	5×10^{-12}	5×10^{-12}	5×10^{-12}
$\alpha\ (dB/m)$	11.6	22	100
$\beta_2(s^2/m)$	-0.1701×10^{-24}	-0.56×10^{-24}	20×10^{-24}
$\gamma_1\ (1/mW)$	12.0968	7.47	9.677
$\gamma_2\ (1/mW)$	7.8125	6.579	6.25

Now we can consider that $\beta_2 = 0$, because β_2 is very small (10^{-24}), and we can change the equation from equations (4.1.6) and (4.1.7) to this form

$$\frac{\partial A}{\partial z} = -\frac{\alpha}{2}A - (A^2 + B^2)[A\gamma_2 + B\gamma_1]. \qquad (4.1.11)$$

$$\frac{\partial B}{\partial z} = -\frac{\alpha}{2}B - (A^2 + B^2)[B\gamma_2 - A\gamma_1]. \qquad (4.1.12)$$

When compensation program values given in Table 1, it produces us the following forms

In Figure (4.2) shows to us the input and output pulse shapes (values 1) after distance 5mm, which the red curve represents the input wave, while showing the linear loss effect α in orange curve and operates a reduction in the value of the input wave, when I add the nonlinear Kerr effect γ_1 to linear loss effect (yellow dash curve) the wave does not show any affected and applies the resulting wave on the orange curve, while the green curve shows us what happens when add tow

photon absorption effect γ_2 with linear loss effect where the reduction will happen to the wave twice resulting from reduction of linear loss effect alone , while at the impact on the wave with $(\alpha\ ,\ \gamma_1\ ,\gamma_2)$, the blue dash curve representative them will apply to the green curve completely.

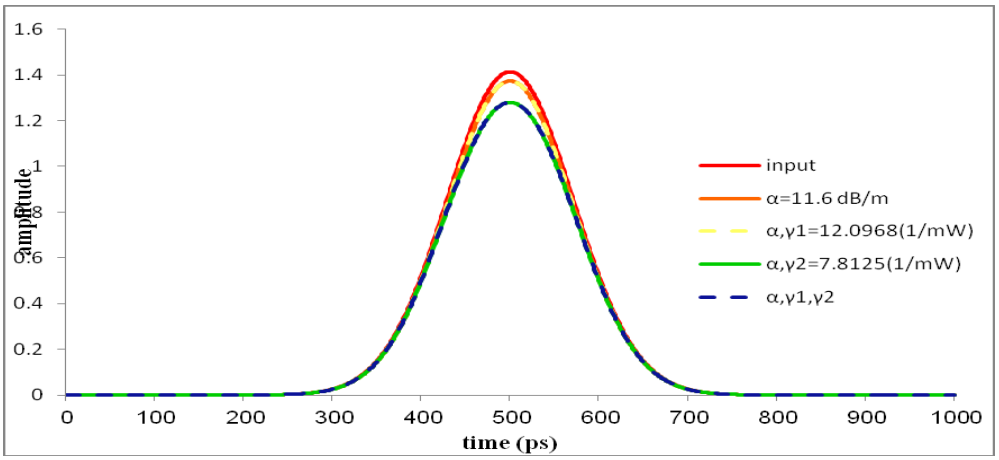

Figure (4.2): The input (red curve) and output pulse shapes (parameter values column1) and the corresponding spectra under several different conditions, orange curve include linear loss (α) only, green curve include linear loss and TPA effect (γ_2), yellow dashed curve include linear loss and nonlinear Kerr effect (γ_1), and blue dashed curve include $(\alpha, \gamma_1, \gamma_2)$.

Now the spread of the incoming wave (values 1) when it moves in the waveguide its length 5 cm after 10 distance steps the Figure (4.3) shows that to us.

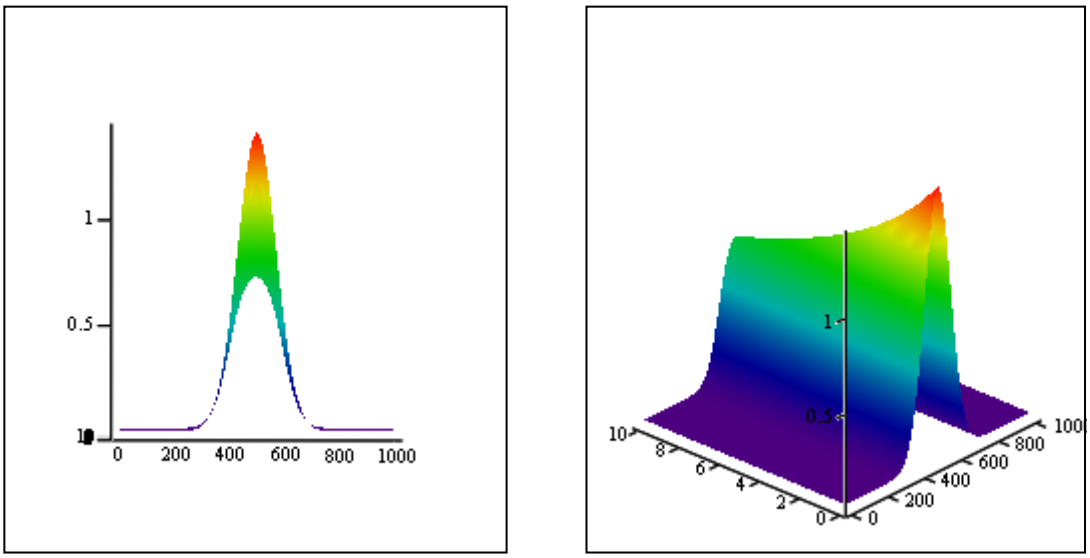

Figure (4.3): the surface shape of the wave when it moves in the waveguide (value 1) its length 5 cm, after 10 distance steps.

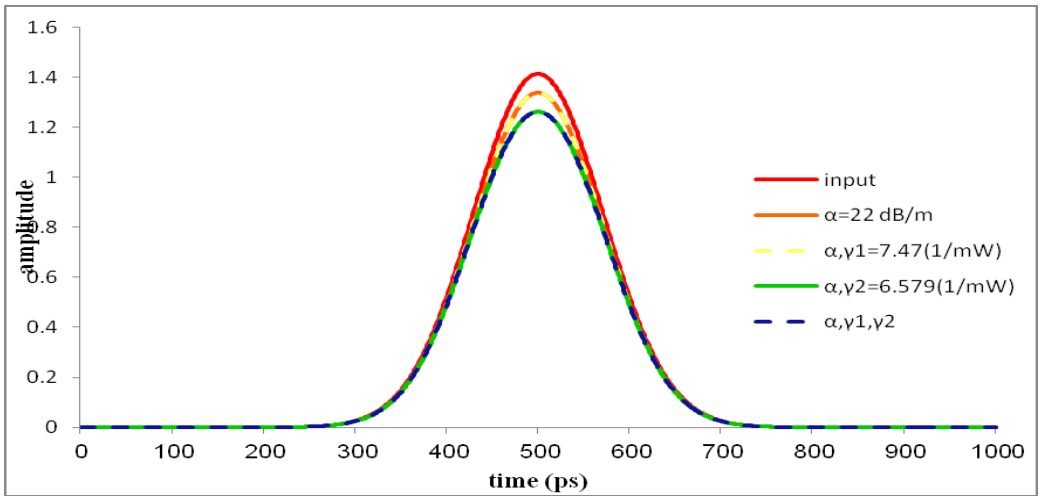

Figure (4.4): The input (red curve) and output pulse shapes (parameter values column 2) and the corresponding spectra under several different conditions orange curve include linear loss (α) only, green curve include linear loss and TPA effect(γ_2), yellow curve include linear loss and nonlinear effect(γ_1), and blue curve include ($\alpha, \gamma_1, \gamma_2$)

Figure (4.4) shows the input and output pulse shapes (parameter values 2) after 5 mm distance, which the red curve represents the input wave while the impact of the linear loss effect α will appear in orange curve which leads to a reduction in the input wave, upon added the nonlinear Kerr effect $\gamma_1$to α as it appears in the dash yellow curve the wave will apply to the orange curve, but if we used the influence of tow photon absorption γ_2 to α as in the green curve, the value of the decrease of the wave will reach almost twice of the resulting from reduction of linear loss effect alone, while at the impact on the wave with (α , γ_1 , γ_2), the dash blue curve representative them will apply to the green curve completely.

Now the spread of the incoming wave (values 2) when it moves in the waveguide its length 5 cm after 10 distance steps the Figure (4.5) shows that to us.

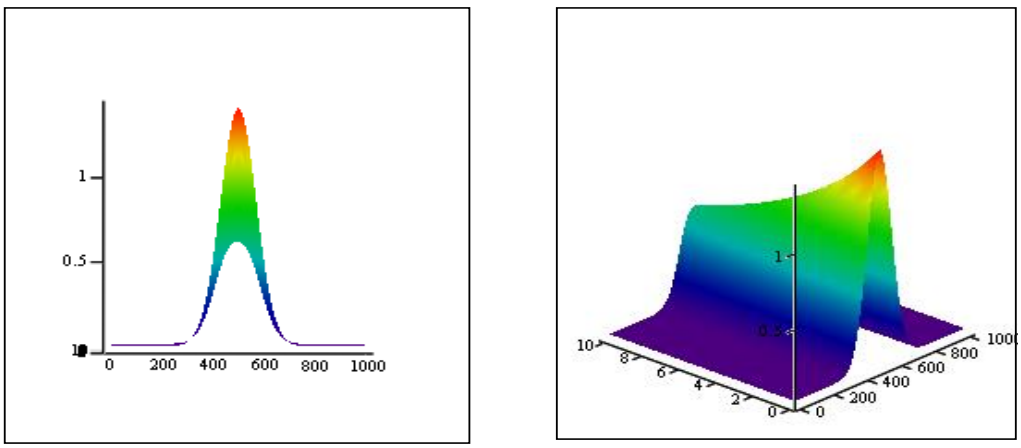

Figure (4.5): the surface shape of the wave when it moves in the waveguide (value 2) its length 5 cm, after 10 distance steps.

$$\begin{cases} \frac{\partial A}{\partial z} = -B\gamma_1(A^2 + B^2). \\ \\ \frac{\partial B}{\partial z} = +A\gamma_1(A^2 + B^2). \end{cases}$$

Figure (4.6) shows the input and output pulse shapes (parameter values 3) after 5 mm distance, which the red curve represents the input wave while the impact of the linear loss effect α will appear in orange curve which have a reduction in the value equivalent almost a quarter of the value of the input wave, upon added the nonlinear Kerr effect γ_1 to α as it appears in the dash yellow curve the wave will apply to the orange curve, but if we used the influence of tow photon absorption γ_2 to α as in the green curve, the value of the decrease of the wave will reach almost a third of the input wave, while at the impact on the wave with (α , γ_1 , γ_2), the dash blue curve representative them will apply to the green curve completely.

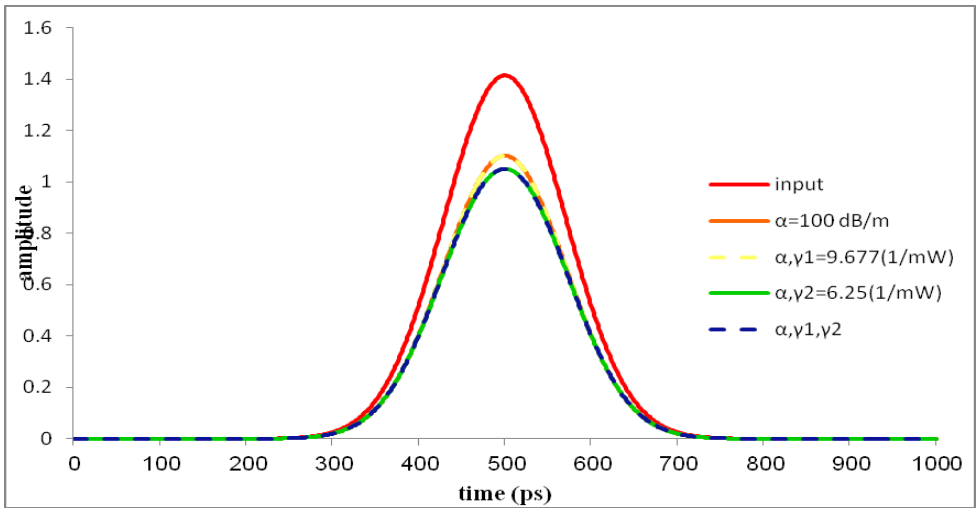

Figure (4.6): the input (red curves) and output pulse shapes (parameter values column 3) and the corresponding spectra under several different conditions, orange curve include linear loss (α) only, green curve include linear loss and TPA effect (γ_2), yellow dash curve include linear loss and nonlinear effect (γ_1), and dash blue curve include$(\alpha, \gamma_1, \gamma_2)$.

Now the spread of the incoming wave (values 3) when it moves in the waveguide its length 5 cm after 10 distance steps the Figure (4.7) shows that to us.

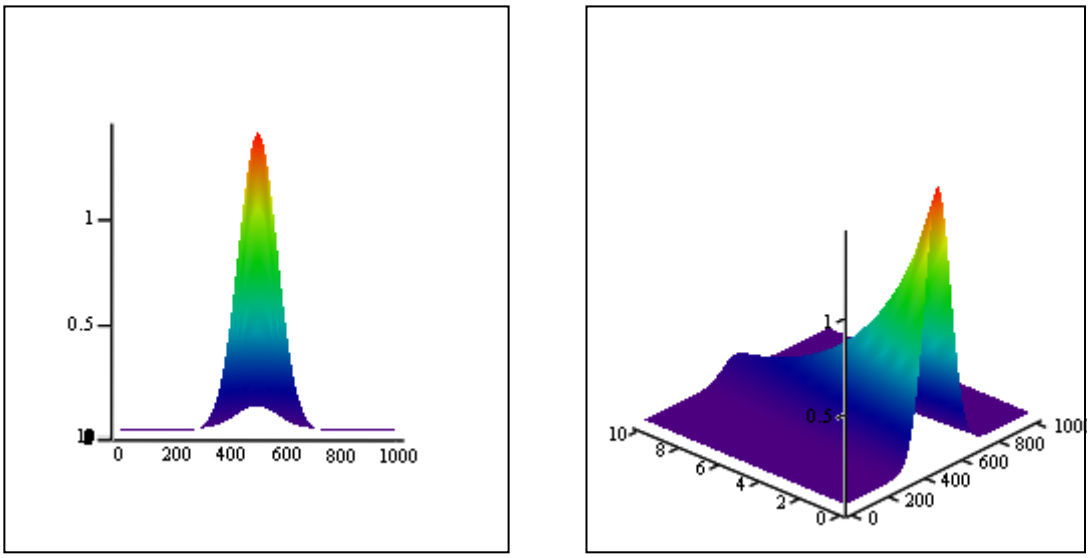

Figure (4.7): the surface shape of the wave when it moves in the waveguide (value 3) its length 5 cm, after 10 distance steps.

from equations (4.1.6) (4.1.7) if we put that $\alpha = 0$, $\beta = 0$ and $\gamma_2 = 0$, we obtain the equations (4.1.13)

These equations show that the real and imaginary parts of the function **F** are mutual in the equations, where each value will replace the other one resulting in pure rotation and hence no reduction in amplitude.

Figure (4.8) shows the effect of γ_1 on the real and imaginary parts of the function **F** where the influence on the absolute value of **F** will have no effect, meaning that its impact will be zero when ($\alpha = 0, \gamma_2 = 0, \beta_2 = 0$).

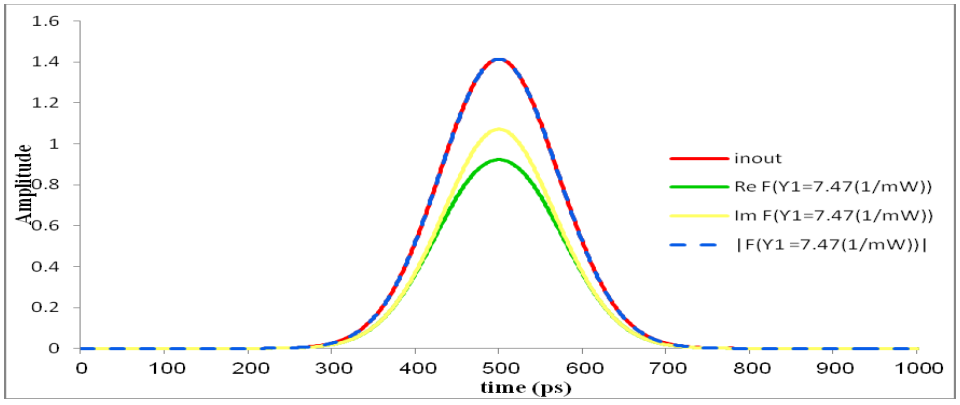

Figure (4.8): The input wave (red curve) and the effect Re**F** ,Im**F**, and an absolute value of **F** (dashed blue curve).

Now, if we will inter a Gaussian shape in other kind of silicon waveguide at $\lambda = 1550nm$ and used the parameters from table (2), and comparable with column (3) from table (1), then we obtain the following figures.

Table (2): values of the parameters for silicon waveguides used for numerical calculations.

Values	(4) [52, 53] *porous silicon*	(5) [54,55] *silicon-nc wg*
$A_{eff}\ (m^2)$	19.3×10^{-12}	0.05×10^{-12}
$n_2\ (m^2/W)$	2.3×10^{-18}	8×10^{-17}
$\beta_{TPA}(m/W)$	0.8×10^{-11}	20×10^{-11}
$\alpha\ (dB/m)$	1100	200
$\beta_2(s^2/m)$	0	0
$\gamma_1\ (1/mW)$	0.0769	1000
$\gamma_2\ (1/mW)$	0.2073	2000

The figure (4.9) shows the spread of the incoming waves when they moves in the waveguide its length 3 mm after 10 distance steps as a comparison between SOI waveguide (column (3) from taple (1)) and porouse silicon (from taple (2)). As shown in figure (b,d) the impact of porous silicon is leads to large reduced on the input wave to become a quarter of value in the end, and figure (a,c) shown the impact of SOI waveguide which the effect on the input wave is small impact after this distance.

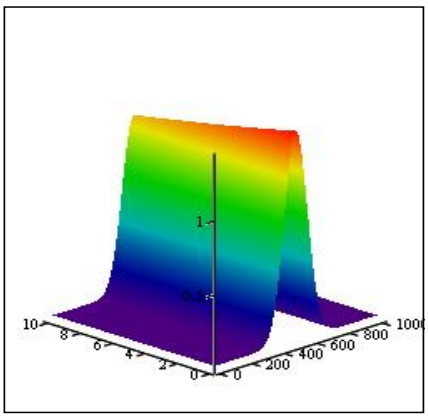

(a)

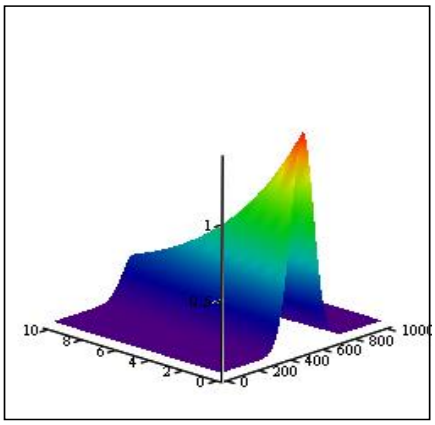

(b)

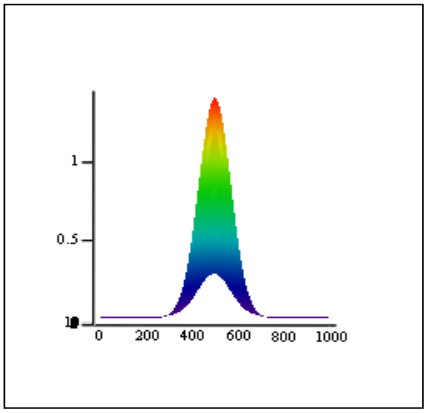

(c)

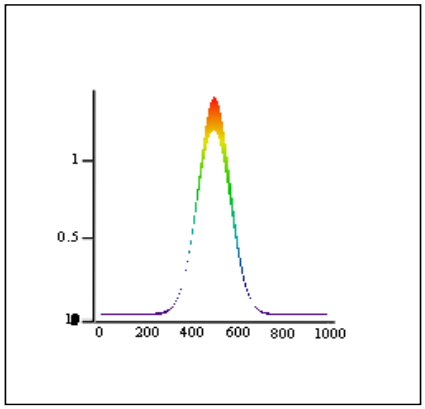

(d)

Figure (4.9): The comparison between the surface shapes of SOI waveguide (a, c) (column (3) from table (1)), and porous silicon (b, d) (table (2)) when they move in the waveguide its length 3mm, after 10 distance steps.

The figure (4.10) shows the spread of the incoming waves when they moves in the waveguide its length 3 mm after 10 distance steps as a comparison between SOI waveguide (column (3) from taple (1)) and silicon nano-crystal deposited by "Plasma Enhanced Chemical Vapor Deposition" method (PECVD) (from taple (2)) . As shown in figure (b,d) the impact of silicon nano-crystal is leads to large reduced on the input wave but with change in the shape to more flattened shape wave, and figure (a,c) shown the impact of SOI waveguide which the effect on the input wave is small impact after this distance.

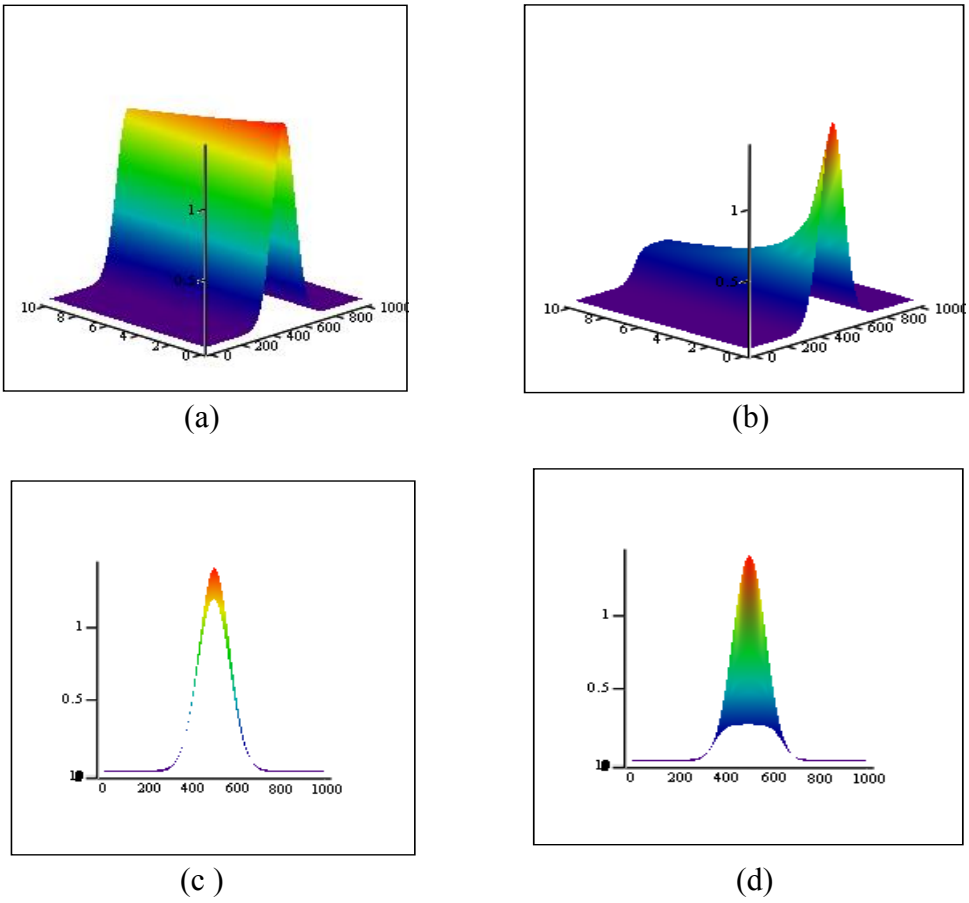

Figure (4.10): The comparable between the surface shapes of SOI waveguide (a, c) (column (3) from table (1)), and silicon nanocrystal (b, d) (table (2)) when they move in the waveguide its length 3mm, after 10 distance steps.

Conclusion

In this paper, the nonlinear Schrödinger equation in time domain and its numerical solutions have been derived and studied numerically with finite difference method up second order. This equation is used to study the propagation of ultra short optical pulses in silicon waveguides and the possibility of soliton formation and supercontinuum generation.

For silicon waveguides its length less that 1cm the Gaussian wave we entered and maintained their shapes so they are considered as soliton or solitary waves. For porous silicon and silicon nano-crystal other physical effects may affect the various parameters and still under experimental investigations.

This paper provides an overview for understanding the basic theory of silicon waveguides, so that the properties of silicon waveguides can be used to new and useful applications in communications and fast optical transmission of data in computers.

References:

[1] Bo Thide,"Electromagnetic field theory", (2nd edition), Dover Publications.
[2] David Halliday, Robert Resnick, Jearl Walker, "Fundamentals of Physics", (4th edition).
[3] Carlo G. Someda, "Electromagnetic waves", (2nd edition), informa Taylor &Francis Group.
[4] S. F. Mahmoud, "electromagnetic Waveguides Theory and Applications", Peter Peregrinus Ltd. London, United Kingdom (1991).
[5] U. A. Bakshi, A. V. Bakshi, "Transmission Lines & Waveguides", (1st edition) Technical Publications Pune (2006).
[6] Gerald. B. Whitham, "Linear and Nonlinear Waves",(Pure and Applied Mathematics: A Wiley Series of Texts, Monographs and Tracts), by John Wiley &Sons, (1999).
[7] Michel Remoissenet, “Waves called solitons concepts and experiments” Springer (1999).
[8] Charles Kittel, “Introduction to Solid State Physics”, (3th edition) John Wiley &sons (1968).
[9] Richard Soref “The Past, Present, and Future of Silicon Photonics”, IEEE Journal, vol. 12, no. 6, (2006)
[10] Govind P. Agrawal, "nonlinear fiber optics", (3rd edition), Academic Press, (1995).
[11] Govind P. Agrawal, “Applications of nonlinear fiber optics”, (2nd edition), Academic Press publications, (2008) .
[12] Govind P. Agrawal, “Highly Nonlinear Fibers and Their Applications”, University of Rochester, (2007).
[13] Nicolaas Bloembergen, "Nonlinear optics: Past, Present, and Future", IEEE Journal, vol.6, no.6, (2000).
[14] Paul M. Peterson, "Frequency Doubling and second order nonlinear optics", technical university of Denmark.
[15] Katsunari okamoto, "Fundamentals of optical waveguides", (2nd edition), Academic Press (2006).
[16] Prof Daniel B. Ostrowsky, "Guided wave nonlinear optics", university of nice (france), (1991).
[17] Robert W. Boyd, “Nonlinear optics”, 3th edition, Academic Press (2008).
[18] Richard L. Sutherland, “Handbook of nonlinear optics”, 2nd edition, Marcel Dekker (New York) (1996).
[19] G. Priem, P. Dumon, P. Bienstman, G. Morthier and R. Baets, “Effect of loss mechanisms on kerr-nonlinear resonator behavious”, Optical society of America (2004).